frontiers | Frontiers in Materials

TYPE Original Research
PUBLISHED 16 August 2023
DOI 10.3389/fmats.2023.1234455

Check for updates

OPEN ACCESS

EDITED BY
Shifa Wang,
Chongqing Three Gorges University, China

REVIEWED BY
Weihua Yang,
Nanjing University of Aeronautics and Astronautics, China
Qian Mao,
The Pennsylvania State University (PSU), United States
Chengshi Gong,
Lanzhou City University, China

*CORRESPONDENCE
Lixiang Jiang,
jlx8972@163.com

RECEIVED 04 June 2023
ACCEPTED 07 August 2023
PUBLISHED 16 August 2023

CITATION
Qiao S, Jiang L, Jiang H, Liu Y, Xu Y, Jiao Z, Cui N and Wang L (2023), Reactive molecular dynamics simulation on the disintegration of Kapton and Upilex-S during atomic oxygen impact.
Front. Mater. 10:1234455.
doi: 10.3389/fmats.2023.1234455

COPYRIGHT
© 2023 Qiao, Jiang, Jiang, Liu, Xu, Jiao, Cui and Wang. This is an open-access article distributed under the terms of the Creative Commons Attribution License (CC BY). The use, distribution or reproduction in other forums is permitted, provided the original author(s) and the copyright owner(s) are credited and that the original publication in this journal is cited, in accordance with accepted academic practice. No use, distribution or reproduction is permitted which does not comply with these terms.

Reactive molecular dynamics simulation on the disintegration of Kapton and Upilex-S during atomic oxygen impact

Shiying Qiao, Lixiang Jiang*, Haifu Jiang, Yuming Liu, Yanlin Xu, Zilong Jiao, Naiyuan Cui and Lu Wang

Beijing Institute of Spacecraft Environment Engineering, Beijing, China

Polyimides are polymeric materials that are widely used in spacecraft applications owing to their unique properties. However, exposure to a low-Earth-orbit environment containing atomic oxygen (AO) results in the disintegration of polymeric materials on the surface of spacecraft, thereby affecting the lifespan. Along with the development of theoretical research, the reactive force-field (ReaxFF) interatomic potential has become a robust computational method for exploring, developing and optimizing the material properties. This study employs the ReaxFF reactive-force-field molecular dynamics simulation (ReaxFF MD) program to investigate and compare the performance of two typical polyimide materials, Kapton and Upilex-S, under the impact of AO. Various aspects such as variations in the temperature, mass loss, decomposition products, and damage propagation depth were examined. Although these materials have similar elemental composition (C/H/O/N), they have different structures. Our results indicate that AO is initially adsorbed on the surfaces of both Kapton and Upilex-S. The continuous impact of AO leads to chemical reactions between AO and Kapton/Upilex-S. Erosion proceeds from the surface toward the interior of the materials. Similar to the findings of Experiment 2 conducted by the Materials International Space Station, our results also reveal that Upilex-S exhibits a lower mass loss and erosion yield than Kapton under the same AO conditions. This difference is primarily attributed to the distinct molecular structures of both Kapton and Upilex-S. Our study could provide valuable technical support for the extensive application of Upilex-S in spacecraft.

KEYWORDS

low Earth orbit, atomic oxygen, LAMMPS, ReaxFF, Upilex-S

Introduction

The disintegration of surface materials on spacecraft during orbital flights remains a significant concern. Particularly, in low-Earth orbit, high-speed collisions of abundant atomic oxygen (AO) in this region with the spacecraft can severely disintegrate the surface materials, thus decreasing the performance, reliability, safety, and ultimately reducing the in-orbit lifespan of the spacecraft (Banks et al., 2004). In low-Earth orbit, the average relative kinetic energy of high-flux AO impacting the spacecraft surface ranges from 4.5 to 5.0 eV. In addition, AO exhibits strong oxidizing properties and is highly corrosive to spacecraft surface materials, particularly polymeric materials (Samwel, 2014;

Zhang et al., 2012; Jiao et al., 2022; Duo et al., 2011). Polyimides, a class of polymers with high overall performance, have excellent mechanical properties, insulating ability, ultraviolet stability, and thermal stability and are lightweight. Therefore, they are widely utilized in the surfaces, thermal control systems, and structures of spacecraft. However, they are highly susceptible to erosion by AO (Banks et al., 1985; Zhao et al., 2010). Both space-borne (Sechkar et al., 2001; Gorreta et al., 2016) and ground-based AO experiments (Miller et al., 2008; Stambler et al., 2009; Aghaei et al., 2017) have been extensively carried out by researchers globally in an effort to protect polyimide materials from disintegration by AO and to enhance the in-orbit lifespan of spacecraft. However, space-borne experiments are costly to launch and have long testing cycles, whereas ground-based AO experiments cannot achieve ideal test conditions owing to the limitations of the experimental equipment, thus affecting the accuracy of the results. Additionally, neither space-borne nor ground-based experiments allow for the observation of the dynamic interaction between AO and materials.

However, with improvements in computational performance and the development of theoretical research, Molecular dynamics (MD) emerges as a powerful tool enabling simulations of diverse materials properties at the atomic scale. Therefore, MD has become an important tool as a complement to experimental studies. Among the many force-fields employed in MD simulations, the reactive force-field (ReaxFF) method developed by van Duin et al. is capable of performing dynamic simulations of bond breakage and formation during chemical reactions in materials (van Duin et al., 2001; Senftle et al., 2016; Nayir et al., 2023). This is a novel and effective approach for simulating the impact of AO on polymeric materials. Moreover, the ReaxFF force-field method enables real-time, dynamic simulations of the interaction between AO and polymeric materials, rather than mere observation of the surface of the studied materials at the macroscopic level after AO impact.

ReaxFF is trained against quantum mechanics principles but maintains computational efficiency similar to classical force fields, enabling simulations of large-scale systems over extended time frames (van Duin et al., 2001; Senftle et al., 2016; Nayir et al., 2023). It has been successfully applied to the research of material pyrolysis, heterogeneous catalysis, atomic layer deposition and carbonization process, etc. But the latest RaexFF application report on C/H/O/N- based polymeric systems which is composed with the same elements of the two polyimide materials studied in this work, is mainly focusing on the carbonization process, such as Kowalik et al. (2019). that basing on the Density Functional Theory (DFT) data——in which, a improved ReaxFF force field is developed containing elements of C/H/O/N (ReaxFF parameters - CHON-2019). Using the improved ReaxFF parameters set, simulations of primary stage of carbonization process for the three polymers of idealized ladder PAN (polyacrylonitrile), a proposed oxidized PAN and PBO(poly(p-phenylene-2,6-benzobisoxazole)) are conducted in the atomic scale, revealing that presence of the amide groups for PAN is important for effective N_2 production, the main products of oxidized PAN are N_2, H_2, H_2O, and the main products of PBO are hydrogen, water and carbon monoxide; besides, it was deemed that PBO polymers would become a promising alternative precursor for carbon fiber productions. Whereas, Zhang et al. (2023) used ReaxFF CHON-2019 parameter set developed by Kowalik exploring the stress graphitization mechanisms of a Carbon nanotube/PAN-based carbon matrix composite, revealing that when the CNT content is higher in the system, the nitrile groups in the PAN matrix are arranged along the CNTs, which subsequently results in preferential dehydrogenation and clustering of carbon rings at 1500K and eventually graphitization of the PAN matrix. Mao et al. (2020). used ReaxFF MD gaining the understanding of functionalities of the oxygen-containing and nitrogen-containing groups in pure and PAN/PBO blend Carbon Fiber precursors, revealing that O-containing groups are more efficient for triggering the carbonization reactions, whereas N-containing groups are far longer retained in the graphitic materials and play a key role in capturing and converting carbon radical species into the graphitic networks. Rajabpour et al. (2021) used ReaxFF MD to study the mechanical properties enhanced atomistic mechanism of graphene included PAN/graphene carbon fibers, which reveals that the graphene edges have a catalytic role and act as seeds for the expedited alignment of all-carbon rings. Mao et al. (2022) used ReaxFF MD developing a series of ReaxFF MD simulations were performed on the carbonization process for ten single and PAN-based blend polymers—it was found that PAN/CL remarkably increases the carbon yield with considerable all-carbon ring structure formation, which could be validated by Raman and TEM test. The above-mentioned reports of ReaxFF application on C/H/O/N-based polymeric systems not only demonstrated the power of ReaxFF technology, but also proved the advanced reliability of ReaxFF through the simulation incorporating with test verification.

There are also many reports, just like this paper, that have used ReaxFF MD to investigate the impact of AO on polymeric materials in spacecraft, and similarly, they have obtained reliable results. For instance, Rahnamoun and van Duin. (2014) conducted pioneering research using ReaxFF MD to study the effects of AO impact on Kapton, POSS, Teflon, and amorphous silica, considering phenomena such as the mass loss and temperature variation, as well as the disintegration products and erosion yield. Among the tested materials, Kapton exhibited the most significant mass loss owing to AO impact, whereas amorphous silica exhibited high stability, These results aligned well with the corresponding experimental findings. Using the ReaxFF MD method, Zeng et al. (2015) investigated the effects of AO impact on PVDF, FP-POSS and the composite of FP-POSS and PVDF. The results demonstrated that the PVDF/FP-POSS composite exhibited higher stability under AO impact than the other evaluated materials. Rahmani et al. (2017) applied ReaxFF MD to investigate the performance of three Kapton-based materials mixed with POSS, graphene, and carbon nanotubes, respectively, under the impact of AO. A significant improvement in the AO resistance was observed for all three modified Kapton materials. Recently, Fu et al. (2021) applied the ReaxFF method to investigate the impact of AO on polyethylene terephthalate (PET). The simulated AO erosion yield of PET is comparable with the data obtained from Materials International Space Station Experiment 2 (MISSE 2) (De Groh et al., 2008). The aforementioned studies collectively demonstrate the significant application potential of

the ReaxFF MD reactive simulation method for investigating the effects of AO on polymeric materials used in aerospace applications.

In this study, we investigated the effects of AO impact on both Kapton and Upilex-S using the ReaxFF MD. Kapton and Upilex-S are typical polyimide materials with excellent properties overall. Aside from their different molecular chain structures, both materials are primarily composed of H, C, O, and N atoms. Additionally, their monomers contain identical numbers of H, C, and N atoms, differing only in the number of oxygen atoms, where Upilex-S contains one less oxygen atom than Kapton. The data obtained from MISSE-2 (De Groh et al., 2008) showed that Upilex-S exhibited a lower AO erosion yield than Kapton. However, Kapton is more commonly used in the aerospace field. Therefore, This raises our strong interest in using ReaxFF MD to study the impact of AO on both materials. We first established models for Kapton and Upilex-S and subsequently used ReaxFF to simulate the effects of AO impact. We then compared and analyzed the erosion behavior of Kapton and Upilex-S under AO impact, focusing primarily on phenomena such as temperature variation and mass loss, as well as the reaction products and damage propagation depth (DPD). This study aims to provide technical insights into the broad-scale application of Upilex-S in the aerospace field.

Simulation methodology

ReaxFF force-field

Conventional polymer force-fields, such as COMPASS, CVFF, CHARMM, and AMBER, are inadequate for simulating the breakage and formation of bonds. Hence, they are unsuitable for examining the impact of AO on polyimide materials. In this study, we employed the ReaxFF force-fields proposed by van Duin et al. Compared to conventional force-fields, ReaxFF determines the connectivity between atoms by calculating the bond order based on the interatomic distances. As chemical bonds break and form, the connectivity between atoms is continuously altered, allowing the simulation of bond breakage and formation throughout the process. Similar to empirical non-reactive force-fields, ReaxFF divides the total energy of the system into different energy contributions. The total energy is expressed by the following equation (van Duin et al., 2001):

$$E_{system} = E_{bond} + E_{triple} + E_{C2} + E_{val} + E_{pen} + E_{tors} + E_{lp} + E_{coa} + E_{conj} + E_{over} + E_{under} + E_{H-bond} + E_{vdW} + E_{Coulomb}$$

Where, E_{system} is the total system energy, E_{bond} is the bond energy term, E_{triple} is the triple bond energy correction term, E_{C2} is the triple bond energy penalty term, E_{val} is the valence angle energy term, E_{pen} is the bond angle energy penalty term, E_{tors} is the torsion angle energy term, E_{lp} is the lone pair energy term, E_{coa} is the three-body conjugate effect energy term, E_{conj} is the four-body conjugate effect energy term, E_{over} is the over alignment energy correction term, E_{under} is the under alignment energy correction term, $E_{H\text{-}bond}$ is the non-bonding hydrogen bonding interaction term, E_{vdW} is the van der Waals energy, $E_{coulomb}$ is the Coulomb energy.

In this equation, all the connectivity-dependent parameters, such as angle and torsion, are related to the bond orders, which are calculated based on the interatomic distances and updated at each iteration. Compared to non-reactive force-fields, ReaxFF calculates non-bonding interactions between each pair of atoms, regardless of their connectivity. The coulomb and van der Waals energy terms incorporate shielding terms to eliminate excessive non-bonding interactions (van Duin et al., 2001; Rahnamoun and van Duin., 2014). More detailed information regarding the ReaxFF is provided in the article by van Duin et al. (2001).

In the present study, the ReaxFF force-field parameters set (CHONSi-2014) proposed by Rahnamoun and van Duin. (2014), including H, N, C, and O elements, were used to simulate the AO impacts on Kapton and Upilex-S. This ReaxFF parameter set has been applied to successfully simulate AO effects on various polymeric materials, including polyimide, yielding reliable research outcomes (Rahnamoun and van Duin., 2014; Zeng et al., 2015; Kim and Choi, 2021).

Simulation models

Simulation models for Kapton and Upilex-S were established prior to the AO impact simulations. The process of constructing the AO erosion models for Kapton and Upilex-S is illustrated in Figures 1, 2. Specifically, we first created monomeric structures for Kapton ($C_{22}H_{12}O_5N_2$) and Upilex-S ($C_{22}H_{12}O_4N_2$). Thereafter, 50 Kapton monomers with a total of 2050 atoms and 50 Upilex-S monomers with a total of 2000 atoms were separately placed in cubic boxes to form amorphous models with an initial density of 0.1 g/cm^3. The systems were then subjected to a 2 ns NPT (constant atomic number, N; constant pressure, P; constant temperature, T) simulation at atmospheric pressure and room temperature (300 K). The pressure and temperature were controlled using a Berendsen barostat and a Nosé–Hoover thermostat (Evans and Hoian, 1985), respectively. Using the NPT simulation, the volume of the cubic boxes was gradually reduced to stabilize the densities of the Kapton and Upilex-S models at approximately 1.389 and 1.333 g/cm^3, respectively, as shown in Figure 3 (close to the actual material densities). The final dimensions of the Kapton and Upilex-S models were 28.5 Å × 28.5 Å × 38.8Å and 28.1 Å × 28.1 Å × 38.2Å, respectively. Table 1 provides detailed information regarding the two models.

Simulation details

After constructing the initial models of Kapton and Upilex-S, MD simulations of AO impact on Kapton and Upilex-S were performed separately using the LAMMPS software. The main process consists of three steps. First, to allow for the insertion of AO, the dimensions of the models in the z-direction were expanded to increase the vacuum region of the surface. Periodic boundary conditions were set in the x- and y-directions of the simulation box, whereas the z-direction was set as a fixed boundary condition. Second, the system was subjected to energy minimization using the conjugate gradient method (Štich et al., 1989), and run for 30 ps under NVT (constant atomic number, N; constant volume, V; constant

10.3389/fmats.2023.1234455

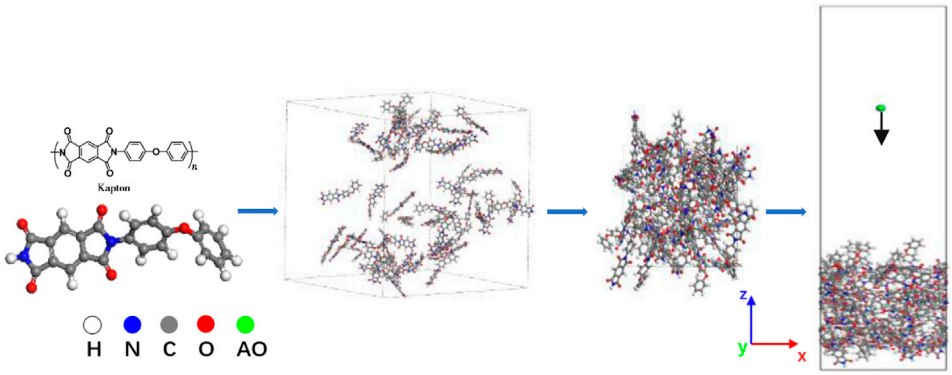

FIGURE 1
Kapton modeling process (the white atoms represent H, the gray atoms represent C, the red atoms represent O, the blue atoms represent N, and the green atom represent AO).

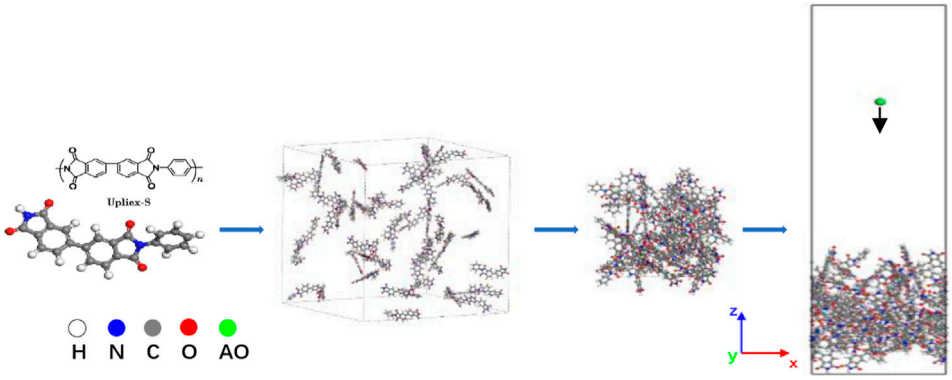

FIGURE 2
Upilex-S modeling process (the white atoms represent H, the gray atoms represent C, the red represent O, the blue atoms represent N, and the green atom represent AO).

temperature, T) conditions at 300 K until a dynamically stable structure with a temperature equilibrium of approximately 300 K was attained for both Kapton and Upilex-S. Third, the system was switched to the NVE (constant atomic number, N; constant volume, V; constant energy, E) simulation, and 150 AOs were randomly inserted at a distance of 74 Å from the material surface at intervals of 200 fs. To simulate the AO impact, the randomly inserted AOs were assigned a velocity of 0.074 Å/fs (~4.5 eV) in a direction perpendicular to the material surface. The time step is set to 0.1 fs, and a total of 300,000 steps (~30 ps) are run under NVE conditions. To prevent a downward drift of Kapton and Upilex-S during the AO impact simulation, the bottom layer of the material was fixed at a height of 10 Å and did not participate in the reaction. The output of the disintegration products was obtained using the "reaxff/species" command in LAMMPS. Atoms were visualized using the Ovito software. A Python program was written to statistically analyze the quantity of the surface dissociation products. Notably, owing to the high computational cost of ReaxFF MD, the number of AO impacts and monomers in the model was determined based on prior experience by Rahnamoun and van Duin, as well as the thickness of the non-penetrating model after AO impact.

Results and Discussion

AO impact

The reaction simulations in the NVE condition are simulations of a non-equilibrium state, indicating that the system is not in an equilibrium state during the 150 AO impact process. In the NVE condition, a random AO with an energy of 4.5 eV was vertically introduced onto the surface of Kapton and Upilex-S along the z-direction every 200 fs, corresponding to an incident AO dose rate of 5 AO/ps. Each material was subjected to the AO impact for 30 ps (150 AOs). Figures 4, 5 illustrate the structural evolution of Kapton and Upilex-S under the AO impact. During the initial stage of the impact, most AOs are adsorbed onto the surfaces of both materials without undergoing any reaction, and only a few AOs are deflected. In the later stages, the erosion of both materials by AO

10.3389/fmats.2023.1234455

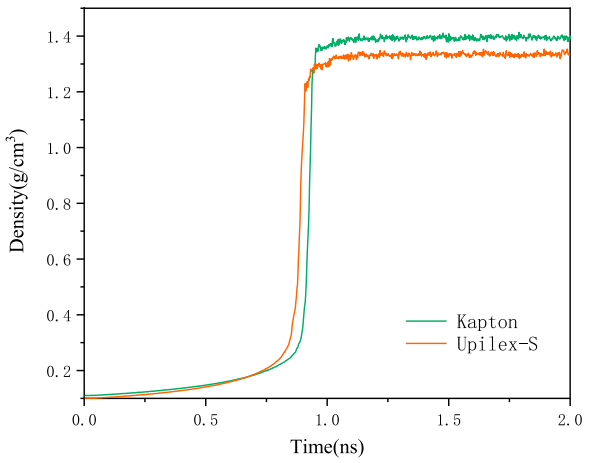

FIGURE 3
Density evolution curves of Kapton and Upilex-S models.

progresses from the surface toward the interior. The matrix that reacts with the AOs possess a loose structure, whereas the matrix that does not react with the AOs undergoes minimal structural changes. Furthermore, more reaction products separated from the surface of Kapton than from the surface of Upilex-S throughout the AO impact process. The resistance of the two materials to AO was investigated by analyzing the temperature variation, mass loss, decomposition products, erosion yield, and damage propagation depth (DPD) under the AO impact.

Temperature evolution and mass loss

In contrast to non-reactive force-fields that can only simulate physical dissociation, reactive force-fields can simulate both chemical and physical dissociation of polymeric materials (Fu et al., 2021). High-speed AO transfers its kinetic energy to the system upon impact, thereby increasing the system temperature. Figure 6A represents the temperature evolution of the Kapton and Upilex-S materials under the AO impact, and illustrates that the temperature of both materials increases almost linearly with the AO impact. The final temperatures of the two materials range from 1,800 to 2,000 K, exhibiting no significant differences. The temperature evolution of AO bombardment on the surface and interior region of Kapton and Upilex-S are respectively illustrated in the Figures 6B, C, which reveals that the temperatures of the interior and surface of the two materials are generally increased in a linear way. However, the temperature of the eroded surface is evidently higher than that in the interior region at any random moment.

TABLE 1 Details of Kapton and Upilex-S models.

System	Chemical structure	Molecular formula	Number of monomer	Density (after 300K NPT)	Model size
Kapton	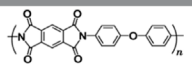	$C_{22}H_{12}O_5N_2$	50	1.389 g/cm^3	28.5 Å × 28.5 Å × 38.8Å
Upilex-S	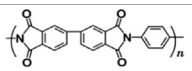	$C_{22}H_{12}O_4N_2$	50	1.333 g/cm^3	28.1 Å × 28.1 Å × 38.2Å

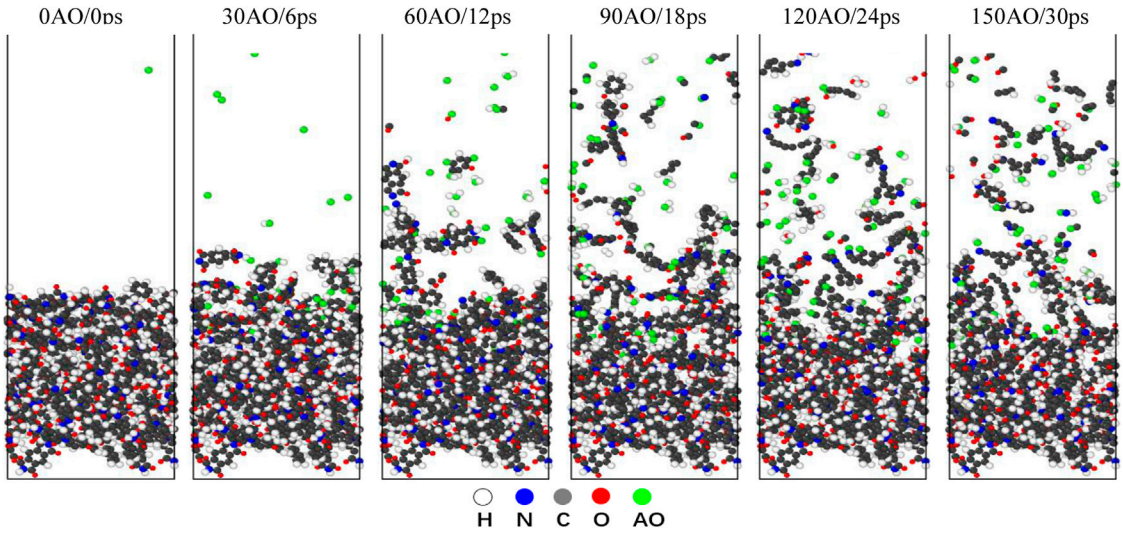

FIGURE 4
Evolution of Kapton structure under 150 AOs impact (the white atoms represent H, the gray atoms represent C, the red atoms represent O, the blue atoms represent N, and the green atom represent AO).

10.3389/fmats.2023.1234455

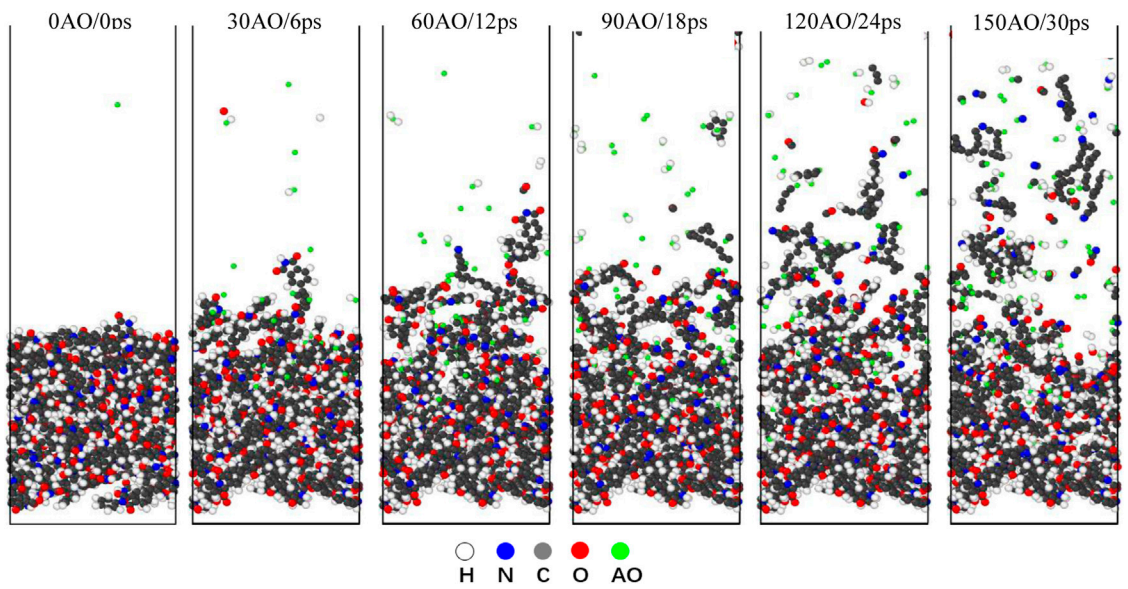

FIGURE 5
Evolution of Upilex-S structure under 150 AOs impact (the white atoms represent H, the gray atoms represent C, the red atoms represent O, the blue atoms represent N, and the green atom represent AO).

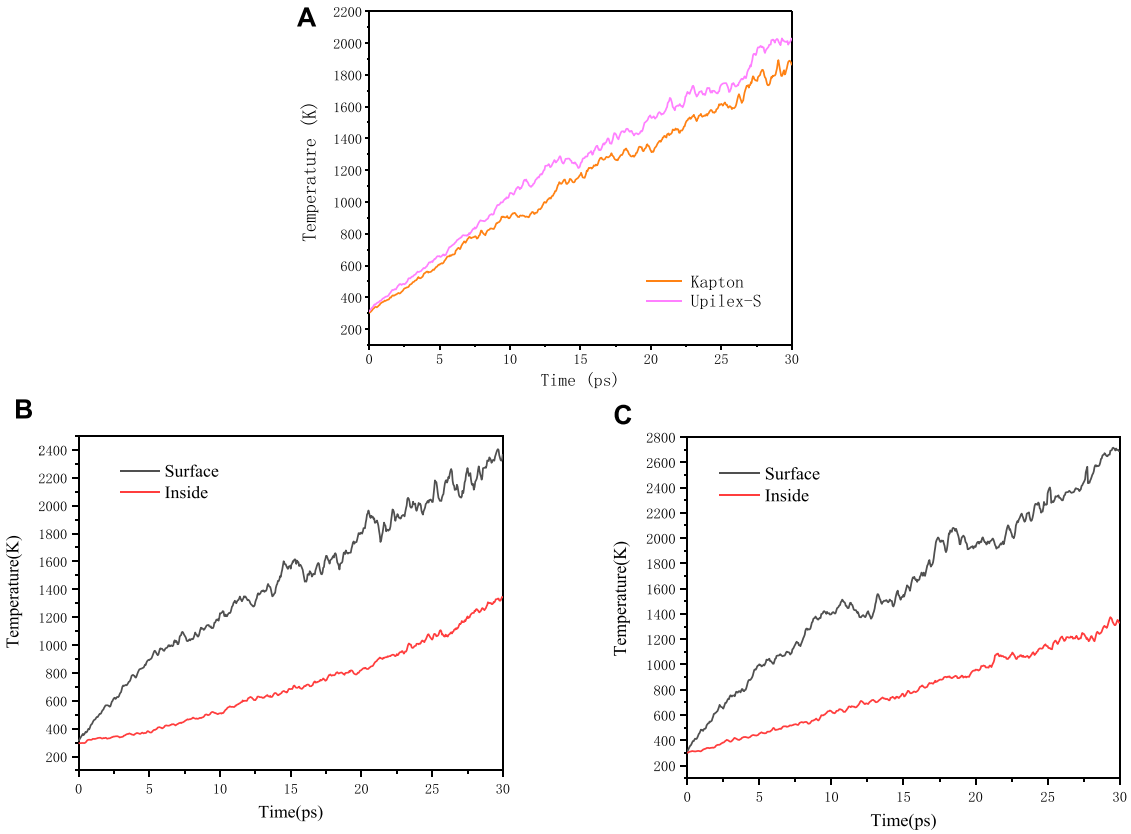

FIGURE 6
(A) The overall temperature evolution of Kapton and Upilex-S under AO impact. **(B)** Temperature evolution of surface and interior region of Kapton under AO impact. **(C)** Temperature evolution of surface and interior region of Upilex-S under AO impact.

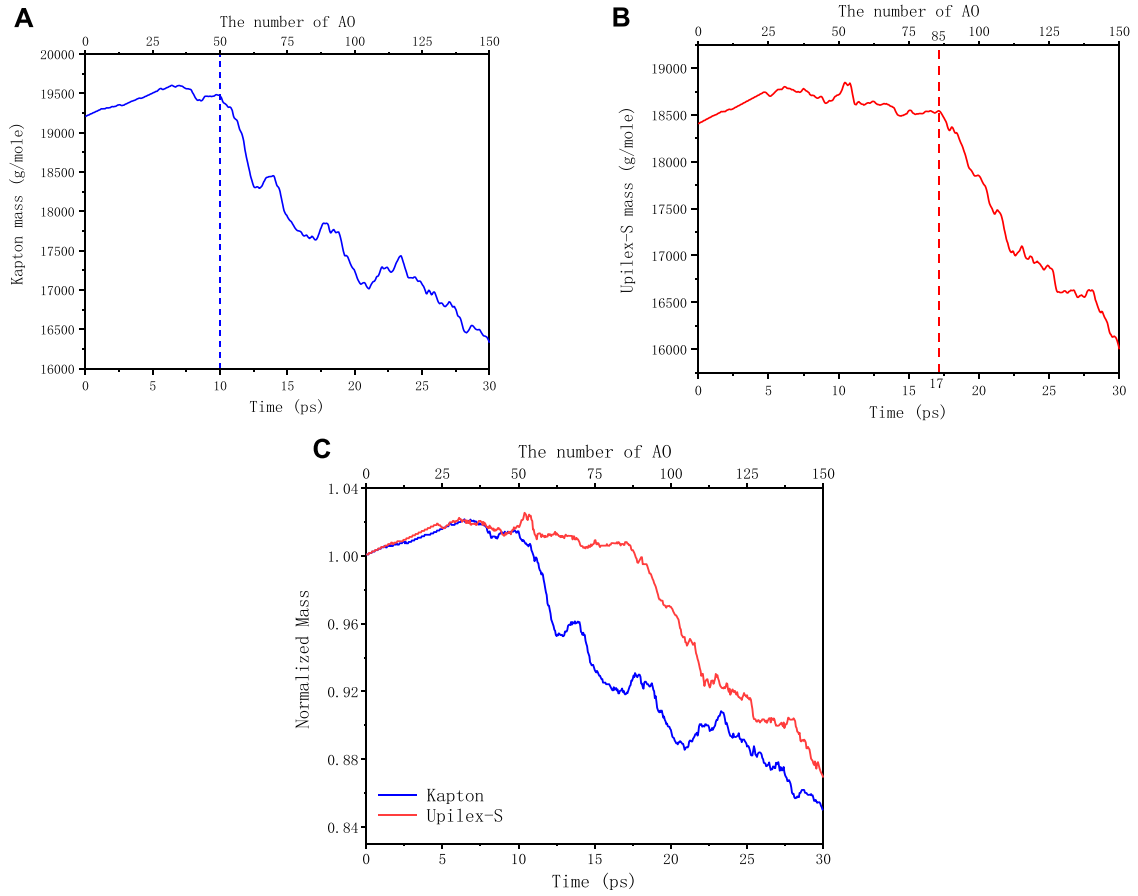

FIGURE 7
(A) Mass evolution of Kapton under AO impact. **(B)** Mass evolution of Upilex-S under AO impac. **(C)** Normalized mass loss of the Kapton and Upilex-S under AO impact.

Figures 7A, B depict the mass changes of the two materials under the AO impact. Within a timeframe of 0–6 ps (0–30 AOs), AO does not chemically react with the surface of either material. Instead, it physically adheres to the material surfaces, increasing their mass. This phenomenon has also been observed in other experimental (Duo et al., 2005) and simulated study (Rahnamoun and van Duin., 2014) on the impact of AO on Kapton. As the number of impacts with AO increases, the surface temperature of the material increases rapidly. This rapid increase in temperature causes strain on the bonds between atoms on the surface, which makes the chemical reactions between the impacting AOs and the surface material more facile. This results in greater release of products and rapid disintegration of the material, leading to rapid mass loss. Both Kapton and Upilex-S exhibit a trend of initial mass increase followed by a decrease. In a similar study where ReaxFF was utilized to investigate the effects of the AO impact on other polymers, Zeng et al. (2015) suggested that in the initial stages of impact, high-energy AO simply transfers energy to the targeted polymer, and as AO continues to collide with the material, the temperature steadily increases. When the surface atoms of the matrix begin to be released, the reaction of the subsequent incident AOs with the remaining matrix is intensified, resulting in accelerated mass loss. The combined observations in Figures 4, 5 and analysis of the data in Figures 7A, B are consistent with the findings of Zeng et al. Under the AO impact, the rate of erosion of both Kapton and Upilex-S accelerates rapidly with increasing temperature because higher temperature promotes the production of more active and reactive atoms, thus facilitating more extensive chemical reactions with the AOs.

Figure 7A illustrates that Kapton undergoes rapid disintegration and exhibits significant mass loss starting at 50 AO impacts. In contrast, Upilex-S begins to degrade rapidly and exhibits mass loss after 85 AO impacts, as shown in Figure 7B. Analyzation on the outcome of “reaxff/species” commands from LAMMPS software shows that, comparing with Kapton, more AOs are physically adsorbed on the surface of Upilex-S during the 6–17 ps impact timeframe. The detached surface products mainly consist of oxygen molecules formed by the interaction of AOs with the Upilex-S surface and other small molecules; therefore, no significant mass loss was observed for Upilex-S. The AO impact simulations utilized the NVE ensemble, representing an isolated system that does not exchange heat with its surroundings. In addition, owing to the limitations imposed by the size of the system and the number of atoms, it is generally accepted that the mass loss during the initial phase of the AO impact (0–20 ps, corresponding to the first 200,000 steps of the simulation) is the best indicator of the

10.3389/fmats.2023.1234455

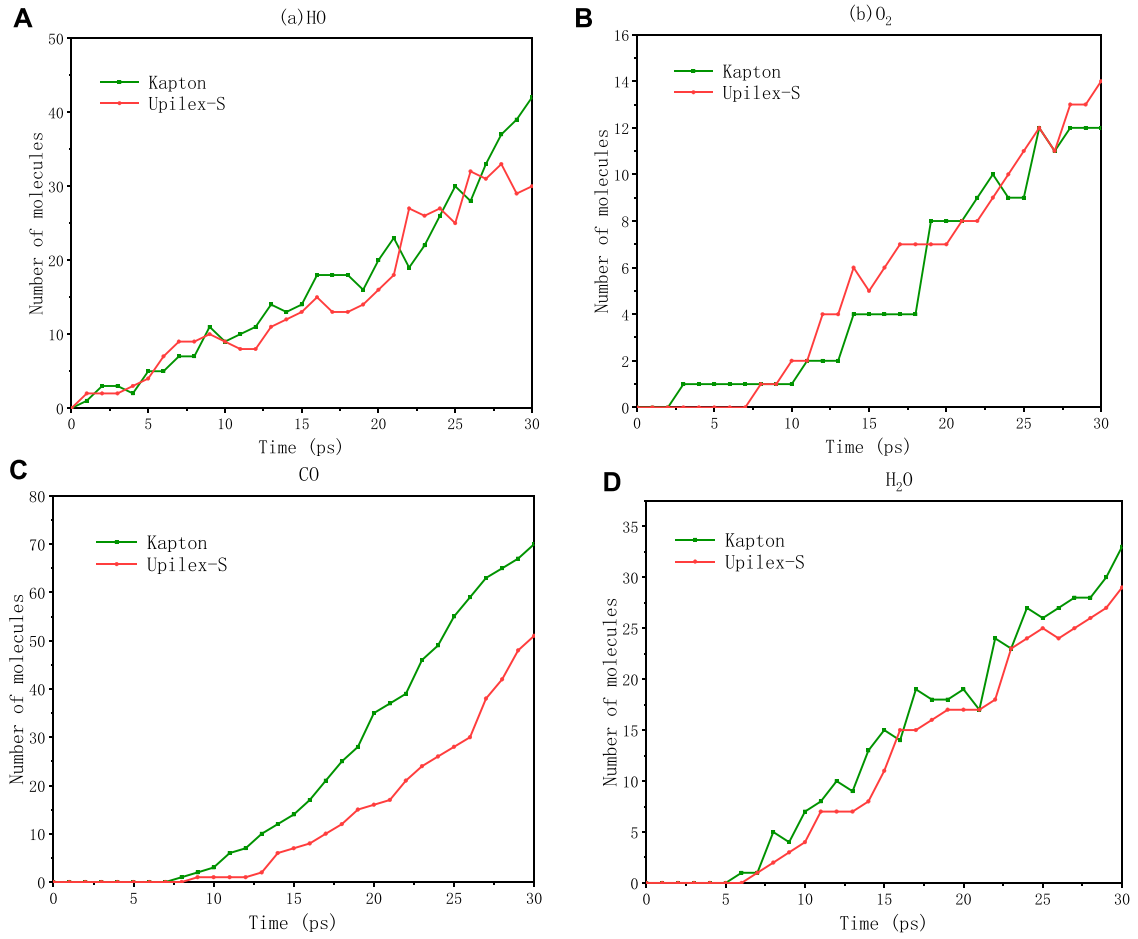

FIGURE 8
Small-molecule production for Kapton and Upilex-S upon bombardment: **(A)** HO, **(B)** O_2, **(C)** CO, **(D)** H_2O.

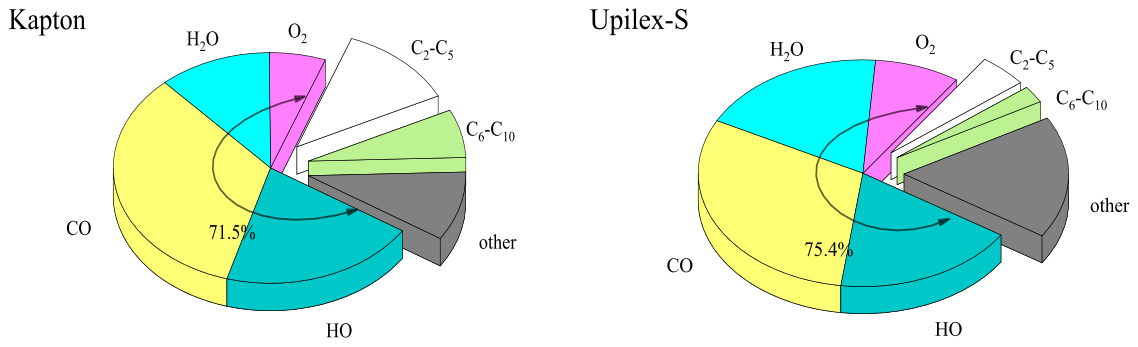

FIGURE 9
The proportions of surface dissociation products from Kapton and Upilex-S after the AO impact.

material performance under the AO impact. Considering the different initial masses of Kapton and Upilex-S, we normalized the mass of each material at any given time during AO impact by dividing it by the initial mass. This enabled us to compare the mass loss of the two materials, as shown in Figure 7C. Figure 7C reveals that during the initial phase of the AO impact, the increase in the mass of the two materials is approximately identical. However, in the later stages of the initial phase, Upilex-S exhibits a smaller mass loss than Kapton. This indicates that Upilex-S is more resistant to the AO impact than Kapton, which is consistent with the findings of the MISSE 2 experiment (De Groh et al., 2008). Both materials display a nearly linear decrease in the mass loss with the continued AO

10.3389/fmats.2023.1234455

TABLE 2 Erosion yield for Kapton and Upilex-S under AO collision.

AO impact time (ps)	Erosion yield ($\times10^{-23}$g/oxygen atom)	
	Kapton	Upilex-S
17	2.23	0.12
18	2.52	0.85
19	2.78	1.51
20	3.27	1.62
Average erosion yield	2.70	1.02

impact. After 150 AO impacts, the degree of mass loss of Upilex-S is similar that of Kapton. Combining with Figure 6 demonstrate that although the temperature changes of the two materials do not differ significantly, Upilex-S consistently maintains a slightly higher temperature than Kapton, particularly in the later stages, which could potentially explain why the mass loss of Upilex-S becomes similar to that of Kapton in the later stages of the AO impact.

The lower mass loss for Upilex-S than that of Kapton during the initial stage of the AO impact can be explained by the bond-dissociation energies (BDEs) (Luo, 2002). The key structural difference between Kapton and Upilex-S is the presence of an additional oxygen atom in Kapton, forming a "C–O–C" structure between the two benzene rings on the main chain. The BDE of the "C–O" bond in the "C–O–C" structure on the main chain is 313.8 kJ/mol (~3.25 eV). In contrast, Upilex-S exhibits a "C–C" bond structure connecting the two benzene rings on the backbone, with a high bond energy of 478.6 ± 6.3 kJ/mol (~5.02 eV). The other bond types in the two materials are identical. Consequently, Upilex-S is more stable under the AO impact than Kapton. Temperature is a macroscopic statistical result of the thermal motion of a large number of microscopic atoms. After the initial phase, as AOs continue to impact the two materials, the temperature increases continuously, leading to highly intense thermal atomic motion in the materials. Atoms with vigorous thermal motion readily react with AO, resulting in a significant mass loss for both materials during the later stages of the AO impact.

Products and erosion yield

After the AO impact, the surface structure undergoes physical disintegration and chemical reactions, with the subsequent separation of the reaction products, resulting in mass loss. Identification and quantification of the reaction products over time present significant challenges in the experiment. However, The determination and quantification of the reaction products are essential parts of the MD ReaxFF research. First, reaction products are directly associated with the mass loss of the material. Furthermore, they provide in-depth insights into the disintegration induced by high-speed AO impacts. In this study, we identified and quantified the substances that were detached from the surface of the materials under the AO impact.

Whether Kapton or Upilex-S, the major small-molecule products that were detached from the surface under the AO impact include HO, O_2, CO, and H_2O. this is because that Kapton and Upilex-S contain the same types of elements and similar atomic bonds. Figure 8 shows the variation in the quantities of the four major products (HO, O_2, CO, and H_2O) over the simulation time. Observation of Figure 8 combined with

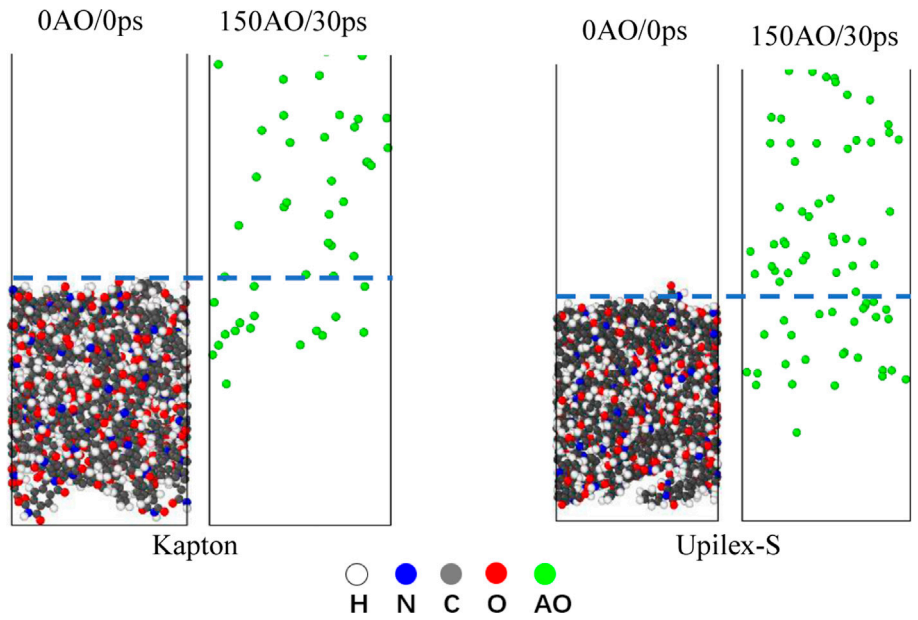

FIGURE 10
Distribution of AO in Kapton and Upilex-S Matrix after AO impact (the white atoms represent H, the gray atoms represent C, the red atoms represent O, the blue atoms represent N, and the green atom represent AO).

10.3389/fmats.2023.1234455

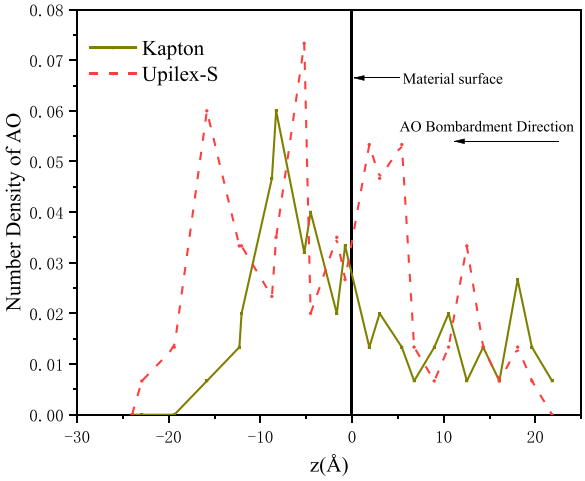

FIGURE 11
Number Density of AO in Kapton and Upilex-S after AO impact. Here, z = 0 Å indicates the initial surface of the material.

TABLE 3 Average Damage Propagation Depth (DPD) with Standard Deviations for Kapton and Upulex-S after the end of the AO impact.

	Kapton	Upilex-S
DPD(Å)	15.22	12.02
Std.dev.(Å)	0.78	0.70

analysis of reaction trajectory files using Ovito software founded that the hydrogen atoms on the benzene rings of both materials initially dissociate and then combine with AO to form hydroxyl radicals (HO), hydroxyl radicals are the dehydrogenation products of both polyimide materials under the AO impact. Comparison of Figures 8A, D shows that H_2O is generated after the formation of the hydroxyl radicals for both materials, In other words, Upon the impact of AO on both materials, hydroxyl radicals (HO) are initially generated. Subsequently, as AO continues to impact, the hydroxyl radicals combine with other hydrogen atoms released from Kapton and Upilex-S to form H_2O molecules. Hydroxyl radicals are precursors to the formation of H_2O molecules. Such a series of formation mechanisms of hydroxyl radicals and water molecules match with the experimentally observed reaction pathways between the reactive AO and hydrogen-containing polymers (Hansen et al., 1965; Medel et al., 2019).

Figure 8B shows the oxygen molecules generated from the surfaces of the two types of materials. One route involves the reaction of oxygen atoms produced from the C=O bond breaking of the imide rings with AO, resulting in the formation of oxygen molecules. Furthermore, O_2 molecules can be formed from the reaction of AOs on the material surface. The carbon atoms in the CO molecules originate from the decomposition of the imide and benzene rings in both Kapton and Upilex-S, As also deduced from Figure 8C, CO is the major reaction product in the AO oxidation process, which is consistent with the experimental observations (Ozawa et al., 2000; Xiao et al., 2010).

Figures 8A, B, D demonstrate that there is no significant difference in the amount of HO, O_2, and H_2O separated from the surfaces of the two materials under the same AO exposure conditions. However, Figure 8C shows that Kapton consistently produces a larger amount of CO than Upilex-S throughout the AO impact period. At the same time, Comparison of Figure 8C and Figures 8A, B, D shows that CO is generated noticeably later than HO, H_2O, and O_2. Based on these two observations, we conclude that there is a relatively lower oxygen atom content of the monomeric structure of Upilex-S than that of Kapton, leading to a deficiency in the oxygen atoms required for CO generation. With Kapton, the extra oxygen atoms responsible for the higher generation of CO molecules originate from the rupture of the C–O–C bonds in the main chain structure, which further

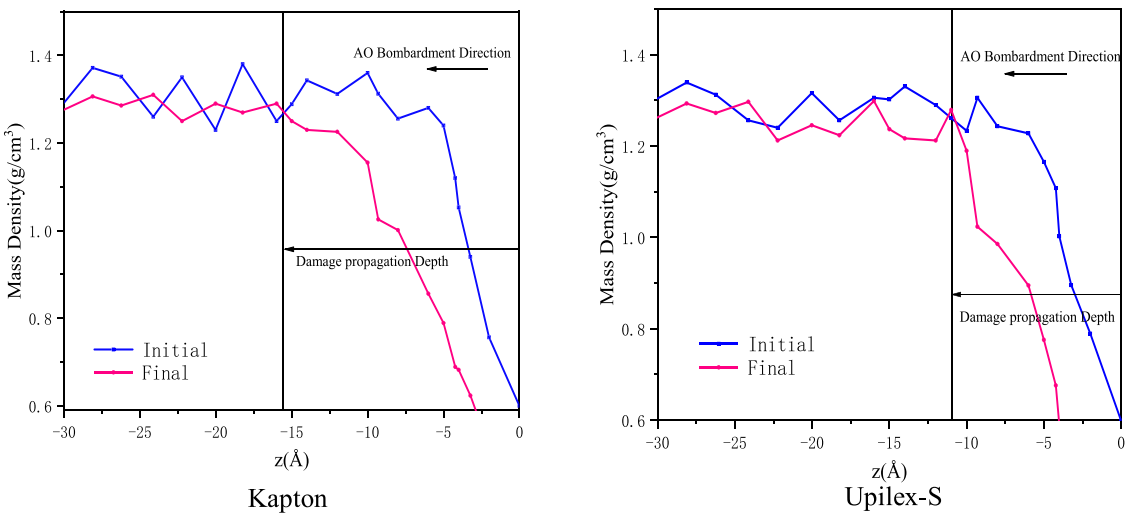

FIGURE 12
Damage propagation depth of Kapton and Upilex-S caused by 150 AO impacts. Here, z = 0 Å indicates the initial surface of the material.

supports the foregoing interpretation. Additionally, the observed order of generation of HO, H_2O, O_2, and CO aligns with the findings of previous studies.

To further analyze the reaction products, we counted the surface separation products of the two materials at the end of the AO impact by major small molecule separations (HO, O_2, CO, H_2O), carbon-chain dissociation products classified based on the carbon content and other dissociation products, and drew a pie chart as shown in Figure 9. The results presented in Figure 9 illustrate that the main small-molecule products, including hydroxyl radicals (HO), oxygen molecules (O_2), carbon monoxide (CO), and water molecules (H_2O), account for 71.5% and 75.4% of the total products from Kapton and Upilex-S, respectively. Upilex-S contains a higher proportion of the main small-molecule products than Kapton, while Kapton has a significantly higher amount of high-carbon-content macromolecular products. As mentioned in previous sections, the backbone of Kapton contains a "C–O–C" bond, while Upilex-S has a higher-energy "C–C" bond that connects the two benzene rings. Under the AO impact, the bond structure of Upilex-S is less prone to breakage, resulting in a lower production of high-carbon-content-macromolecules. Consequently, the mass loss of Upilex-S is insignificant.

The erosion yield is defined as the average mass or volume loss of a material induced by a single AO interaction and serves as an important indicator for studying the effects of AO interactions on spacecraft materials. The data obtained from MISSE 2 (De Groh et al., 2008) reveal that the average AO erosion yield for Kapton is 4.28×10^{-24} g/atom, which is ~3.35 times that of Upilex-S (1.28×10^{-24} g/atom). In this study, Upilex-S exhibits a noticeable mass loss after 17 ps of AO exposure. So Table 2 lists the AO erosion yield of Kapton and Upilex-S from 17 to 20 ps. According to Table 2, it can be observed that the average erosion yield of Kapton is 2.6 times that of Upilex-S. Considering that in the low-Earth-orbit (LEO) environment, material degradation is influenced by AO and other environmental factors in space. Meanwhile, heat exchange with the external environment is not considered in this simulation. The stabilized density in the model is slightly lower than the density of the actual material. Additionally, limitations are imposed by the model size and number of atoms. Hence, the simulated erosion yield is deemed reasonable.

AO penetration depth and damage propagation depth

It is extremely difficult to experimentally characterize the AO penetration depth and AO-induced damage depths of the materials. However, MD simulations are effective for studying the AO penetration and damage propagation depths. To further analyze the degradation of Kapton and Upilex under the AO impact, we plotted the visual representations of the AO penetration depth using the Ovito software (Figure 10) and the number density distribution of AOs after 150 AO impacts (Figure 11). Figure 10 shows that AO penetration is deeper in Upilex-S than in Kapton. Furthermore, more AOs are retained in the Upilex-S matrix than in Kapton. Figure 11 confirms that the maximum penetration depths of the AOs in Upilex-S and Kapton are 22.9 Å and 15.8 Å, respectively. Additionally, Upilex-S has a higher AO number density and a higher peak value than Kapton. These findings indicate that Kapton is more stable than Upilex-S under the AO impact, contradicting the aforementioned findings in previous sections, while being in line with the notion that deeper AO penetration typically corresponds to more severe damage. Therefore, following the approach adopted by Rahmani et al. (2017), we further analyzed the damage propagation depth (DPD) of Kapton and Upilex-S after 150 AO impacts.

The DPD is determined by the change in the initial and final mass densities along the z-axis (parallel to the direction of the AO impact). It is defined as the distance between the initial surface and the depth where the final mass density starts to remarkably decrease compared with the initial mass density of the material. For the accuracy of the DPD results, we conducted two additional AO impact simulations separately for each material and calculated the average and standard deviation of the DPD based on the three AO impact simulations. Figure 12 presents the DPD of Kapton and Upilex-S induced by 150 AO impacts in the first simulation. Table 3 provides the average and standard deviation of DPD obtained from three simulations. It can be observed that the average DPD is 15.22 Å for Kapton and 12.02 Å for Upilex-S, indicating that Upilex-S is more stable than Kapton under the AO impact, which is consistent with the analysis of the normalized mass loss and major products. The observations in Figures 10, 11 are attributed to the low density of Upilex-S. Although the AO penetration depth is an important indicator, assessment of the AO resistance based solely on this factor may not produce reliable results, which is an interesting finding.

Conclusion

ReaxFF is a comparatively novel force-field method that can be used to simulate the breakage and formation of bonds between atoms in a system. In this study, ReaxFF MD was applied to investigate and compare the performance of two polyimide materials, Kapton and Upilex-S, under the AO impact. The results demonstrate that the masses of Kapton and Upilex-S first increase and subsequently decrease. Specifically, during the initial stages of the AO impact, AOs are physically adsorbed onto the surfaces of both materials. With continuous AO impact and increasing temperatures, rapid chemical degradation occurs. Furthermore, the erosion of Kapton and Upilex-S proceeds inward from the surface. The structures that undergo chemical reactions with AO become loose, whereas those that are not subjected to AO erosion change only minimally.

The simulated mechanisms of HO and H_2O generation under the AO impact are consistent with the relevant experimental findings, indicating that the formation of H_2O molecules requires HO as a precursor. Consistent with the results obtained from MISSE-2, this study confirms that Upilex-S exhibits a lower mass loss and a lower AO erosion rate under the AO impact than Kapton. According to the BDE analysis, as well as the analysis of the changes in the quantities of the major reaction products and the proportion of all final reaction products, we conclude that the molecular structure of Upilex-S, which contains a higher-energy C–C bond connecting two benzene rings instead of the C–O–C backbone of Kapton, primarily accounts for the higher stability of Upilex-S under the AO impact. Further, our results demonstrate that material

damage cannot be reliably assessed using only the AO penetration depth. This study not only demonstrates the significant potential and high reliability of the ReaxFF MD in investigating the effects of the AO impact on spacecraft materials but also provides a technical reference for the application of Upilex-S in spacecraft.

Data availability statement

The raw data supporting the conclusion of this article will be made available by the authors, without undue reservation.

Author contributions

SQ: Investigation, Modeling building, Experiment design, Data curation, Write code, Data analysis, Writing-Original and editing. LJ: Investigation, Experiment design, Data curation, Data analysis, Funding acquisition. HJ: Revision, Write code. YL: Data curation, YX: Investigation. ZJ: Experiment design. NC: Investigation, LW: Investigation, Revision. All authors contributed to the article and approved the submitted version.

Funding

The work was supported by the Key Laboratory of China National Defense Science and Technology Administration (Y-JC-XX-ZH-05).

Conflict of interest

The authors declare that the research was conducted in the absence of any commercial or financial relationships that could be construed as a potential conflict of interest.

Publisher's note

All claims expressed in this article are solely those of the authors and do not necessarily represent those of their affiliated organizations, or those of the publisher, the editors and the reviewers. Any product that may be evaluated in this article, or claim that may be made by its manufacturer, is not guaranteed or endorsed by the publisher.

References

Aghaei, A. A., Eshaghi, A., and Karami, E. (2017). Silicon solar cell performance deposited by diamond like carbon thin film Atomic oxygen effects. *Acta Astronaut.* 138, 369–373. doi:10.1016/j.actaastro.2017.06.016

Banks, B, A., Mirtich, M, J., Rutledge, S, K., and Swec, D, M. (1985). Sputtered coatings for protection of spacecraft polymers. *Thin Solid Films* 127, 107–114. doi:10.1016/0040-6090(85)90216-0

Banks, B. A., de Groh, K. K., and Miller, S. K. (2004). Low earth orbital atomic oxygen interactions with spacecraft materials. *MRS Proc.* 851. doi:10.1557/proc-851-nn8.1

De Groh, K. K., Banks, B. A., Mccarthy, C. E., Rucker, R. N., Roberts, L. M., and Berger, L. A. (2008). MISSE 2 PEACE polymers atomic oxygen erosion experiment on the international space station. *High. Perform. Polym.* 20 (4-5), 388–409. doi:10.1177/0954008308089705

Duo, S., Song, M., Liu, T., and Hu, C. (2011). Effect of atomic oxygen exposure on polyhedral oligomeric silsesquioxane/polyimide hybrid materials in low earth orbit environment. *Key Eng. Mater.* 492, 521–524. doi:10.4028/www.scientific.net/KEM.492.521

Duo, S. W., Li, M. S., Zhang, Y. M., and Zhou, Y. C. (2005). Mass change and erosion mechanism of the polyimide film during atomic oxygen exposure. *Chin. J. Mat. Res.* 19, 337–342.

Evans, D. J., and Holian, B. L. (1985). The nose–hoover thermostat. *J. Chem. Phys.* 83 (8), 4069–4074. doi:10.1063/1.449071

Fu, Y., Peng, F., Zhang, C., Sun, C., Zeng, Z., and Fang, G. (2021). Multi-faceted simulation of atomic oxygen erosion of deorbit sail for cleaning space debris. *Acta Astronaut.* 187, 61–69. doi:10.1016/j.actaastro.2021.06.016

Gorreta, S., Pons-Nin, J., López, G., Figueras, E., Jové-Casulleras, R., Araguz, C., et al. (2016). A CubeSAT payload for *in-situ* monitoring of pentacene degradation due to atomic oxygen etching in LEO. *Acta Astronaut.* 126, 456–462. doi:10.1016/j.actaastro.2016.06.028

Hansen, R. H., Pascale, J. V., De Benedictis, T., and Rentzepis, P. M. (1965). Effect of atomic oxygen on polymers. *J. Polym. Sci. Part A general Pap.* 3 (6), 2205–2214. doi:10.1002/pol.1965.100030609

Jiao, Z., Jiang, H., and Jiang, L. (2022). The test conditions in the study of synergistic effects of atomic oxygen and far ultraviolet irradiation in low Earth orbit. *Spacecr. Environ. Eng.* 39, 230–236. doi:10.12126/see.2022.03.002

Kim, Y., and Choi, J. (2021). Thermal ablation mechanism of polyimide reinforced with POSS under atomic oxygen bombardment. *Appl. Surf. Sci.* 567, 150578. doi:10.1016/j.apsusc.2021.150578

Kowalik, M., Ashraf, C., Damirchi, B., Akbarian, D., Rajabpour, S., and Van Duin, A. C. (2019). Atomistic scale analysis of the carbonization process for C/H/O/N-based polymers with the ReaxFF reactive force field. *J. Phys. Chem. B* 123 (25), 5357–5367. doi:10.1021/acs.jpcb.9b04298

Luo, Y. R. (2002). *Handbook of bond dissociation energies in organic compounds*. Florida: CRC Press.

Mao, Q., Rajabpour, S., Kowalik, M., and van Duin, A. C. (2020). Predicting cost-effective carbon fiber precursors: unraveling the functionalities of oxygen and nitrogen-containing groups during carbonization from ReaxFF simulations. *Carbon* 159, 25–36. doi:10.1016/j.carbon.2019.12.008

Mao, Q., Rajabpour, S., Talkhoncheh, M. K., Zhu, J., Kowalik, M., and Van Duin, A. C. (2022). Cost-effective carbon fiber precursor selections of polyacrylonitrile-derived blend polymers: carbonization chemistry and structural characterizations. *Nanoscale* 14 (17), 6357–6372. doi:10.1039/D2NR00203E

Medel, A., Treviño-Reséndez, J., Brillas, E., Meas, Y., and Sirés, I. (2019). Contribution of cathodic hydroxyl radical generation to the enhancement of electro-oxidation process for water decontamination. *Electrochimica Acta* 331, 135382. doi:10.1016/j.electacta.2019.135382

Miller, S. K. R., Banks, B. A., and Waters, D. L. (2008). Investigation into the differences between atomic oxygen erosion yields of materials in ground-based facilities and LEO. *High. Perform. Polym.* 20 (4-5), 523–534. doi:10.1177/0954008308089711

Nayir, N., Mao, Q., Wang, T., Kowalik, M., Zhang, Y., Wang, M., et al. (2023). Modeling and simulations for 2D materials: a ReaxFF perspective. *2D Mater.* 10, 032002. doi:10.1088/2053-1583/acd7fd

Ozawa, T., Arii, T., and Kishi, A. (2000). Thermogravimetry and evolved gas analysis of polyimide. *Thermochim. Acta* 352-353, 177–180. doi:10.1016/s0040-6031(99)00464-5

Rahmani, F., Nouranian, S., Li, X., and Al-Ostaz, A. (2017). Reactive molecular simulation of the damage mitigation efficacy of POSS-Graphene- and carbon nanotube-loaded polyimide coatings exposed to atomic oxygen bombardment. *ACS Appl. Mater. Interfaces* 9 (14), 12802–12811. doi:10.1021/acsami.7b02032

Rahnamoun, A., and Van Duin, A. C. T. (2014). Reactive molecular dynamics simulation on the disintegration of Kapton, POSS polyimide, amorphous silica, and Teflon during atomic oxygen impact using the reaxff reactive force-field method. *J. Phys. Chem. A* 118 (15), 2780–2787. doi:10.1021/jp4121029

Rajabpour, S., Mao, Q., Gao, Z., Talkhoncheh, M. K., Zhu, J., Schwab, Y., et al. (2021). Low-temperature carbonization of polyacrylonitrile/graphene carbon fibers: a combined ReaxFF molecular dynamics and experimental study. *Carbon* 174, 345–356. doi:10.1016/j.carbon.2020.12.038

Samwel, S,W. (2014). Low earth orbital atomic oxygen erosion effect on spacecraft materials. *Space Res. J.* 7, 1–13. doi:10.3923/srj.2014.1.13

Sechkar, E., Tollis, G., Dever, J., Miller, S., and Messer, R. (2001). Exposure of polymer film thermal control materials on the materials international space station experiment (MISSE). *AIAA* 2001. doi:10.2514/6.2001-4924

Senftle, T. P., Hong, S., Islam, M. M., Kylasa, S. B., Zheng, Y., Shin, Y. K., et al. (2016). The ReaxFF reactive force-field: development, applications and future directions. *Npj Comput. Mater.* 2 (1), 15011. doi:10.1038/npjcompumats.2015.11

Stambler, A. H., Inoshita, K. E., Roberts, L. M., Barbagallo, C. E., de Groh, K. K., Banks, B. A., et al. (2009). Ground-laboratory to in-space atomic oxygen correlation for the PEACE polymers. *AIP Conf. Proc.* 1087. doi:10.1063/1.3076865

Štich, I., Car, R., Parrinello, M., and Baroni, S. (1989). Conjugate gradient minimization of the energy functional: a new method for electronic structure calculation. *Phys. Rev. B* 39 (8), 4997–5004. doi:10.1103/physrevb.39.4997

Van Duin, A. C. T., Dasgupta, S., Lorant, F., and Goddard, W. A. (2001). ReaxFF: a reactive force field for hydrocarbons. *J. Phys. Chem. A* 105 (41), 9396–9409. doi:10.1021/jp004368u

Xiao, F., Wang, K., and Zhan, M. (2010). Atomic oxygen erosion resistance of polyimide/ZrO_2 hybrid films. *Appl. Surf. Sci.* 256 (24), 7384–7388. doi:10.1016/j.apsusc.2010.05.077

Zeng, F., Peng, C., Liu, Y., and Qu, J. (2015). Reactive molecular dynamics simulations on the disintegration of PVDF, FP-POSS, and their composite during atomic oxygen impact. *J. Phys. Chem. A* 119 (30), 8359–8368. doi:10.1021/acs.jpca.5b03783

Zhang, L., Kowalik, M., Mao, Q., Damirchi, B., Zhang, Y., Bradford, P. D., et al. (2023). Joint theoretical and experimental study of stress graphitization in aligned carbon nanotube/carbon matrix composites. *ACS Appl. Mater. Interfaces* 15, 32656–32666. doi:10.1021/acsami.3c03209

Zhang, L., Liu, Y., and Dong, S. (2012). The effect of atomic oxygen on spacecraft materials and the protection measures. *Spacecr. Environ. Eng.* 29, 185–190. doi:10.3969/j.issn.1673-1379.2012.02.014

Zhao, W., Li, W., Liu, H., and Zhu, L. (2010). Erosion of a polyimide material exposed to simulated atomic oxygen environment. *Chin. J. Aeronautics* 23, 268–273. doi:10.1016/s1000-9361(09)60215-6